1 **Supporting Information**

Primary and secondary emissions from a modern fleet of city buses

4 Liyuan Zhou[1,2#], Qianyun Liu[2,a#], Christian M. Salvador[3,b], Michael Le Breton[3,c], Mattias Hallquist[3], Jian
5 Zhen Yu[4] and Chak K. Chan[1,2*], Åsa M. Hallquist[5*]

7 [1] Division of Physical Sciences and Engineering, King Abdullah University of Science and Technology, Thuwal, Saudi Arabia
8 [2] School of Energy and Environment, City University of Hong Kong, Hong Kong SAR, China
9 [3] Department of Chemistry and Molecular Biology, University of Gothenburg, Gothenburg, Sweden
10 [4] Division of Environment and Sustainability, Hong Kong University of Science and Technology, Hong Kong, China
11 [5] IVL Swedish Environmental Research Institute, Gothenburg, Sweden
12 [a] now at: RELX Science Center, Shenzhen RELX Tech. Co,. Ltd., Shenzhen, China
13 [b] now at: Environmental Sciences Division, Oak Ridge National Laboratory, Oak Ridge, TN 37830, USA
14 [c] now at: FEV Sverige AB, Gothenburg, Sweden

15
16
17 [#] The authors contribute equally.

18 *Correspondence to*: Åsa M Hallquist (asa.hallquist@ivl.se); Chak K. Chan (chak.chan@kaust.edu.sa)

19

20   Text S1. Mass-to-charge ratio (m/z) calibration.

21   In this study, six isolated ion peaks (O_2^-, CNO^-, $C_3H_5O_3^-$, $C_2F_3O_3^-$, $C_5F_9O_2^-$, $C_{10}HF_9O_4^-$) were identified as suitable for m/z

22   calibration over the entire studied m/z range. Accuracies are reported as parts-per-million of the m/z value (ppm), calculated

23   as:

24   Accuracy [ppm] = $(m/z_{comp} - m/z_{cal})/(m/z_{cal}) \times 10^6$,   (1)

25   where m/z_{comp} is the peak position, m/z_{cal} is the calibration value. The average accuracy achieved for all six m/z calibrants was

26   within 3 ppm (Table S1), determined from a weighted average of all m/z calibration accuracies and their standard deviations.

27   The accuracy for ions not used in the m/z calibration is also evaluated. Several overlapping peaks are recorded at most integer

28   m/z, and multi-peak fitting is performed to determine individual signal intensities (Figure S3). This procedure may introduce

29   additional uncertainty in the determined peak positions beyond the m/z accuracy of isolated peaks. To estimate the accuracy

30   for the measured ions, multi-peak fits of peaks with known individual peak positions were performed. Table S2 shows the

31   average biases and m/z accuracies for five (Cl^-, NO_2^-, NO_3^-, $C_3H_5O_3^-$, $C_8H_{15}O_2^-$) ions, determined from a time series of several

32   hours of individual spectra. The table lists values for both isolated peaks and those in multiple-peak groups. The average

33   accuracies estimated for the isolated peaks are similar to those for the m/z calibration peaks, but larger for the multiple peak

34   cases, reflecting the additional uncertainties due to the proximity of other peaks.

35

36   Text S2. OH exposure in Go:PAM.

37   The OH_{exp} in Go:PAM was calculated using the model described by Watne et al. (2018). Briefly, a chemical model containing

38   a comprehensive description of ozone photolysis and HO_x chemistry and a skeleton description of NO_x, CO, HC and SO_x

39   chemistry was used to mimic the gas-phase chemistry in Go:PAM (Table S3). The minimum OH exposure was derived for

40   each bus passage plume using the maximum NO_x, HC and CO concentrations in Go:PAM and the corresponding water and

41   ozone concentrations. The assumed speciation of HC was aldehydes (26%), alkanes (33%), alkenes (14%) and aromatic

42   compounds (27%). The oxidation capacity of Go:PAM was offline calibrated by SO_2 as described by Lambe et al. (2011),

43   where the photon flux at 254 nm, $P_{FLUX254}$= 1.57×10^{16} cm^{-2} s^{-1}, and first order loss rates of OH were derived by matching the

44   measured and modeled SO_2 and O_3 decreases.

45   Recently, a concern of non-OH chemistry in the OFR has been raised. (Peng et al., 2016) In this study, we estimated the ratios

46   of exposures of non-OH species to OH exposure for O_3, $O(^1D)$ and $O(^3P)$. The relative importance of non-OH chemistry was

47   evaluated according to Peng et al. (Peng et al., 2016), by taking toluene as a surrogate as it is a common SOA precursor found

48   in vehicle emissions (Gentner et al., 2017; Liu et al., 2019). The undesired VOC destructions by O_3, $O(^1D)$ and $O(^3P)$ were

49   negligible (close to 0 %). The direct photolysis of aromatics in Go:PAM has been evaluated by Watne et al. (2018) under

50   similar experimental conditions (photon flux, residence time). No reductions of toluene and trimethyl-benzene were observed

51   with UV light on.

52

53   Text S3. Classification of acetate-CIMS measured species.

54   The identities of the organic compounds are assigned based on knowledge of the sensitivities of the ionization scheme and the

55   expected compounds emitted from the buses. These compounds were classified into nine families on the basis of their

56   molecular characteristics, according to Liu et al. (2017). Briefly, the functional group composition of ions containing C, H or

57   O atoms was estimated from its elemental composition using the number of oxygen atoms (n_o) and double bound equivalency

58   (DBE, calculated as $1+n_c-1/2n_H$), assuming (1) each ion has at least one carboxylic acid group, (2) the excess oxygen ($n_o - 2$)

59   is contained in hydroxy or keto groups, (3) the excess DBE (DBE − 1) is due to keto groups (priority) or alkene groups, and

60   (4) a phenyl group exists if DBE ≥ 5. The ions are categorized into acid classes using the following prioritized criteria: (1) if

61   DBE ≥ 5, the ion is categorized as an aromatic acid, otherwise (2) if $n_o = 2$, the ion is assigned as a monoacid (either saturated

62   (DBE=1) or unsaturated (DBE>1)), (3) if $n_o > 2$, and $n_o > 2 \times$ DBE, the ion is counted as a hydroxy acid, (4) in the case of n_o

63   > 2 and $n_o \leq 2 \times$ DBE (DBE ≥ 2), the ions is defined as a carbonyl acid if n_o is an odd number, otherwise the ion is referred to

64   as a diacid or hydroxycarbonyl acid. For ions containing N or S atoms, (1) if the $n_N > 0$, and $n_S = 0$, ions is assigned as a nitrogen

65   (N)-containing compounds (no S), (2) if the $n_S > 0$, and $n_N = 0$, ions is assigned as a sulfur (S)-containing compounds (no N),

66   (3) if the $n_N > 0$, and $n_S > 0$, ions is assigned as a N and S-containing compounds. Table S4 lists the classification for the ions

67   identified in this study.

68

69

70
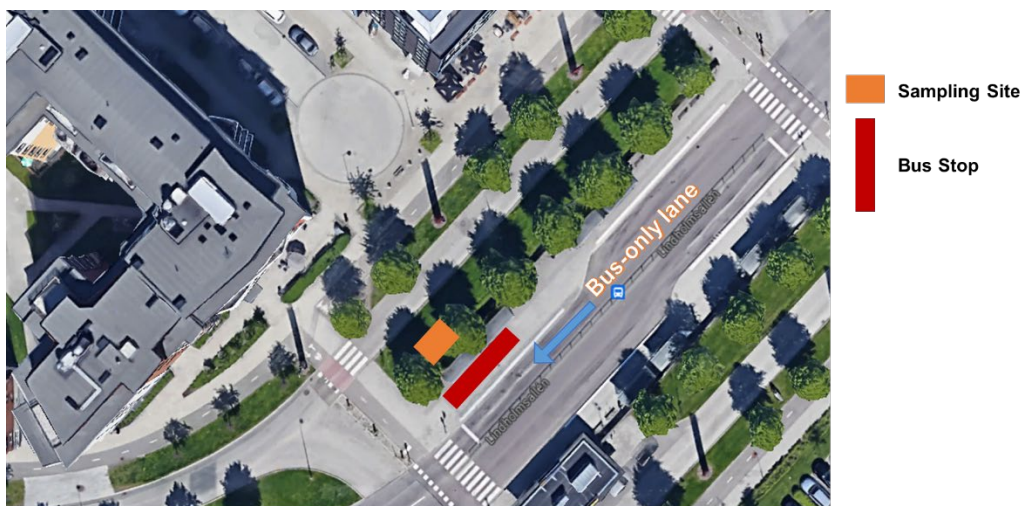
Figure S1. Satellite image of the roadside sampling site at Lindholmen, Gothenburg, Sweden. Map data: © Google, DigitalGlobe.

72

73

74
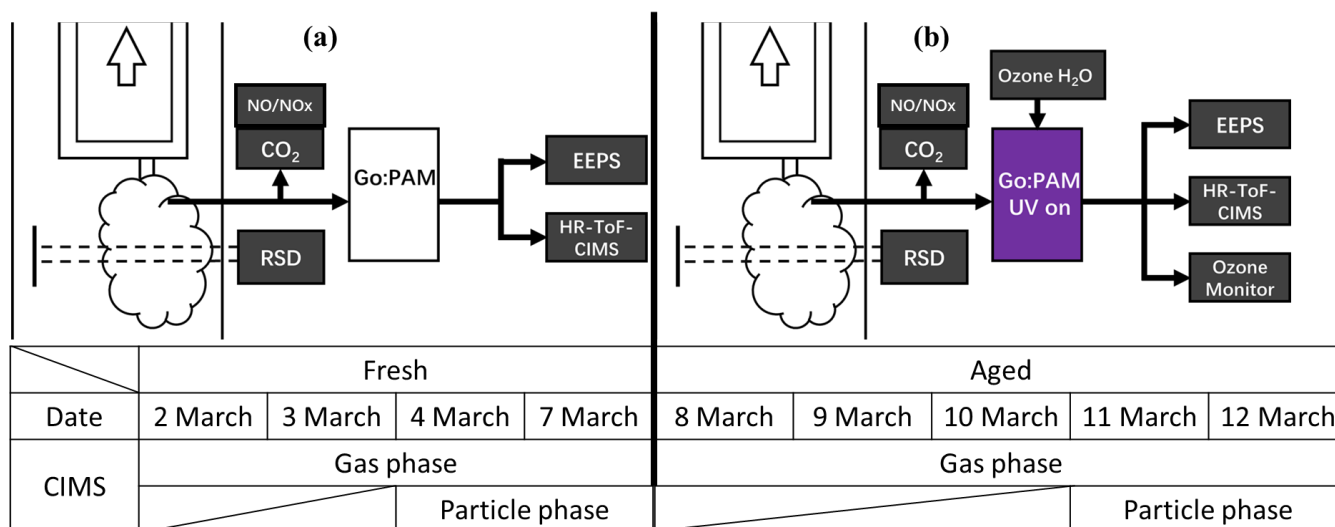
Figure S2. Schematic of the roadside measurement. (a) fresh emission measurements, (b) aged measurements: photo-oxidation of bus plumes. RSD (Remote Sensing Device), CO_2 analyzer, NO/NO_x analyser, EEPS (Engine Exhaust Particle Sizer), and HR-ToF-CIMS (high-resolution time-of-flight chemical-ionization mass spectrometer).

78
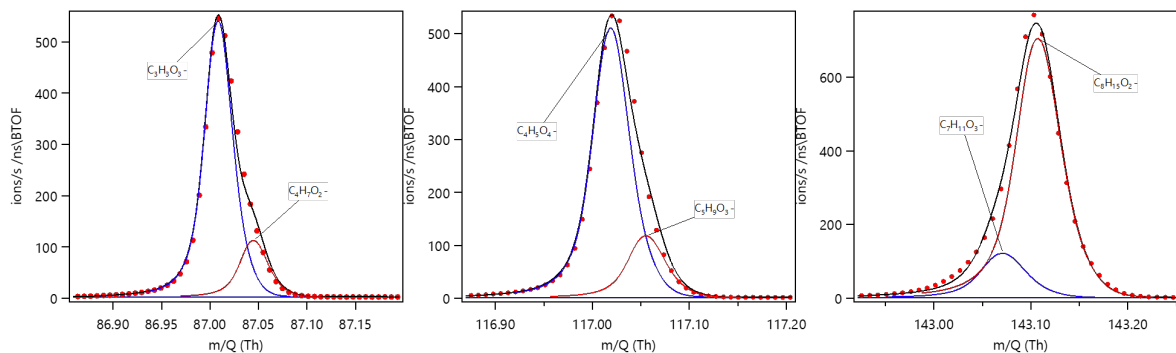
79

80   Figure S3. Example peak fits of major ions.

81
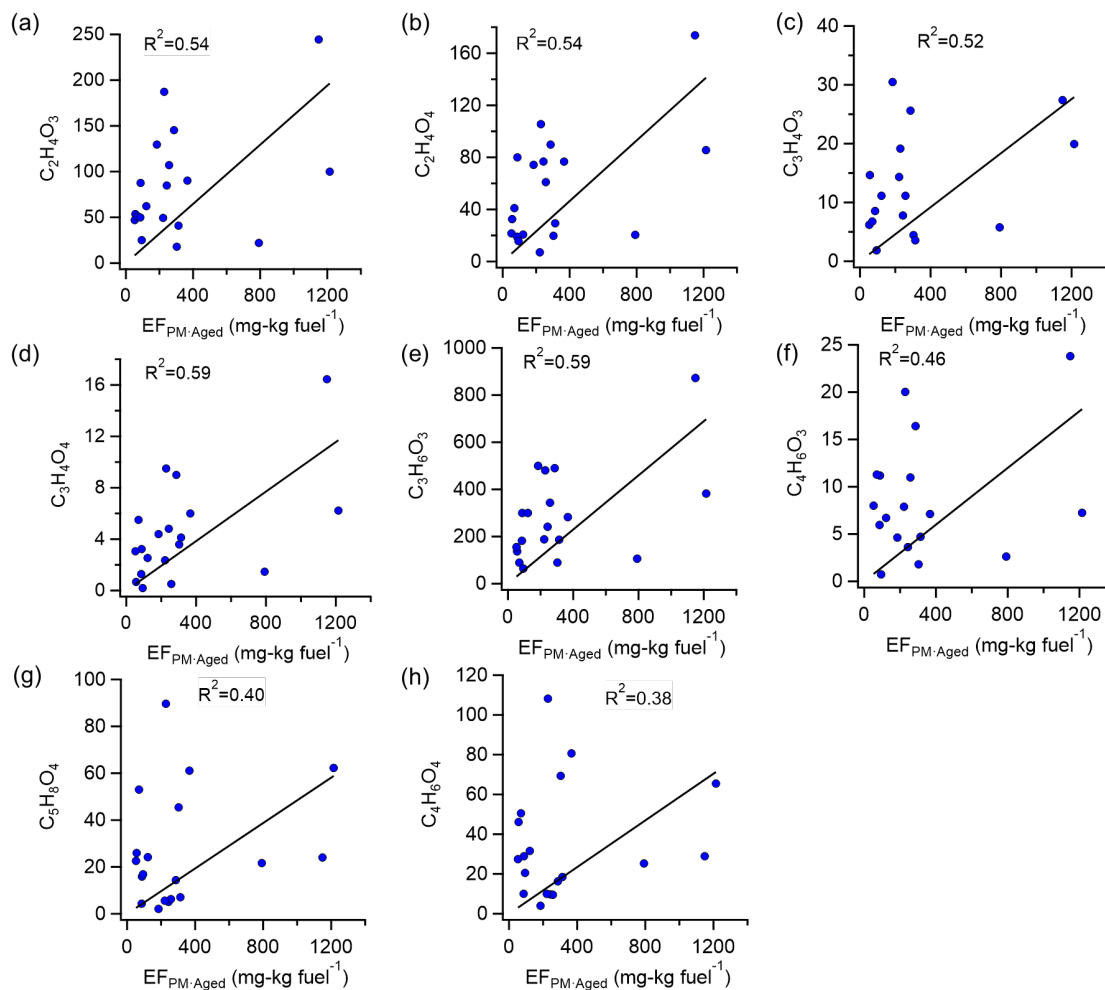
82

83   Figure S4. Correlations between ion counts of most abundant gas-phase organic acids and EF$_{PM:aged}$ (a-h) from 19 buses after
84   oxidation in the Go:PAM.

85

86   Table S1. Isolated ion peaks for m/z calibration.

Exact, m/z	Assigned formula	Accuracy$\pm1\sigma$ (ppm)
31.990378	O_2-	0.2±0.1
41.998537	CNO-	2.6±1.1
89.024418	$C_3H_5O_3-$	2.9±2
112.985587	$C_2F_3O_3-$	3.2±2.7
262.976007	$C_5F_9O_2-$	3.1±1

87

88

89   Table S2. The average biases and m/z accuracies for five ions (determined from a time series of several hours of individual
90   spectra).

Exact, m/z	Assigned formula	Accuracy±1 (ppm)	Comments
34.969401	Cl-	3.7±3.2	Isolate peak
89.024418	$C_3H_5O_3-$	1.5±1.2	Isolate peak
61.988366	NO_3-	1.2±1	Isolate peak
45.993452	NO_2-	2.8±1.2	Isolate peak
143.107753	$C_8H_{15}O_2-$	3.7±5	Multi-peak

91

92

93

94

95   Table S3. Reactions and rate coefficients for model calculations of OH exposure. The data were taken from the literature as
96   described in Watne et al. * 74% of measured HC, **26% of measured HC.

No.	Reaction	k (cm^3 molecule^{-1} s^{-1})
1	$O_3+h\nu \rightarrow O_2+O(^1D)$	0.18
2	$O(^1D)+H_2O \rightarrow OH+OH$	1.99×10^{-10}
3	$O(^1D)+O_2 \rightarrow O(^3p)+O_2$	3.97×10^{-11}
4	$O(^1D)+O_3 \rightarrow O_2+O(^3p)+ O(^3p)$	1.2×10^{-10}
5	$O(^1D)+O_3 \rightarrow O_2+ O_2$	1.2×10^{-10}
6	$O(^1D)+N_2 \rightarrow O(^3p)+N_2$	3.11×10^{-11}
7	$O(^3p)+O_2+M \rightarrow O_3+M$	6.1×10^{-34}
8	$O(^3p)+O_3 \rightarrow O_2+O_2$	7.96×10^{-15}
9	$O(^3p)+OH \rightarrow H+O_2$	3.29×10^{-11}
10	$H+O_2 \rightarrow HO_2$	9.57×10^{-13}
11	$H+HO_2 \rightarrow OH+OH$	7.2×10^{-11}
12	$H+HO_2 \rightarrow O(^3p)+H_2O$	1.6×10^{-12}
13	$H+HO_2 \rightarrow H_2+O_2$	6.9×10^{-12}
14	$OH+OH \rightarrow H_2O+O(^3p)$	1.8×10^{-12}

15	$OH+OH \rightarrow H_2O_2$	6.29×10^{-12}
16	$OH+O_3 \rightarrow HO_2+O_2$	7.25×10^{-14}
17*	$HO_2+HO_2 \rightarrow H_2O_2+O_2$	3.28×10^{-12}
18**	$HC+OH \rightarrow 0.7RO_2+0.3HO_2$	1.0×10^{-11}
19	$HCHO+OH \rightarrow H_2O+CO+HO_2$	9.2×10^{-12}
20	$SO_2+OH \rightarrow OHSO_2$	9.59×10^{-13}
21	$OHSO_2+O_2 \rightarrow SO_3+HO_2$	4.3×10^{-13}
22	$NO+O(^3p) \rightarrow NO_2$	1.66×10^{-12}
23	$NO_2+hv \rightarrow NO+O(^3p)$	1.64×10^{-4}
24	$NO_2+OH \rightarrow HNO_3$	1.06×10^{-11}
25	$NO_2+OH \rightarrow HOONO$	1.79×10^{-12}
26	$HO_2+NO \rightarrow NO_2+OH$	8.16×10^{-12}
27	$RO_2+NO \rightarrow RO+NO_2$	9×10^{-12}
28	$O(^1D)+N_2+M \rightarrow N_2O+M$	2.82×10^{-36}
29	$N_2O+O(^1D) \rightarrow N_2+O_2$	5.09×10^{-11}
30	$N_2O+O(^1D) \rightarrow NO+NO$	7.64×10^{-11}
31	$O(^3p)+HO_2 \rightarrow OH+O_2$	5.87×10^{-11}
32	$O(^3p)+H_2O_2 \rightarrow OH+HO_2$	1.7×10^{-15}
33	$H+O_3 \rightarrow OH+O_2$	2.89×10^{-11}
34	$HO_2+O_3 \rightarrow OH+O_2+O_2$	1.93×10^{-15}
35	$HO_2+OH \rightarrow H_2O+O_2$	1.11×10^{-10}
36	$H_2O_2+hv \rightarrow OH+OH$	1.05×10^{-3}
37	$HO_2+hv \rightarrow OH+O(^1D)$	4.07×10^{-3}
38	$OH+H_2O_2 \rightarrow HO_2+H_2O$	1.8×10^{-12}
39	$NO+O_3 \rightarrow NO_2+O_2$	1.95×10^{-14}
40	$O(^1D)+H_2 \rightarrow OH+H$	1.2×10^{-10}
41	$OH+H_2 \rightarrow H_2O+H$	6.67×10^{-15}
42	$NO_2+O(^3p) \rightarrow NO+O_2$	1.03×10^{-11}
43	$NO_2+O(^3p) \rightarrow NO_3$	1.61×10^{-12}
44	$H+NO_2 \rightarrow NO+OH$	1.28×10^{-10}
45	$NO+NO_3 \rightarrow NO_2+NO_2$	2.65×10^{-11}
46	$NO_2+O_3 \rightarrow NO_3+O_2$	3.2×10^{-17}
47	$CO+OH \rightarrow CO_2+H$	2.4×10^{-13}
48	OH deposition/loss	35
49	$CH_3O \rightarrow HCHO+HO_2$	9.92×10^{3}
50	$CH_3OH+OH \rightarrow HO_2+HCHO$	8.95×10^{-13}
51	$OH+CH_3OOH \rightarrow HCHO+OH$	4.01×10^{-12}
52	$OH+CH_3OOH \rightarrow CH_3O_2$	6.02×10^{-12}
53	$CH_3O_2+CH_3O_2 \rightarrow CH_3OH+HCHO$	4.43×10^{-13}
54	$CH_3O_2+CH_3O_2 \rightarrow CH_3O+CH_3O$	2.58×10^{-13}
55	$CH_3O_2+NO_2 \rightarrow CH_3O_2NO_2$	5.88×10^{-12}
56	$CH_3O_2NO_2 \rightarrow CH_3O_2+NO_2$	1.50
57	$OH+CH_4 \rightarrow CH_3O_2$	6.37×10^{-15}
58	$CH_3O_2+HO_2 \rightarrow CH_3OOH$	4.74×10^{-12}
59	$CH_3O_2+HO_2 \rightarrow HCHO$	4.67×10^{-13}
60	$CH_3O_2+NO \rightarrow CH_3O+NO_2$	7.69×10^{-12}

97

98

99

100

101

102

103   Table S4. Classification of acetate-CIMS measured species.

Elemental composition	Formula	Assigned category
No N or S	DBE=1-3, n_o=2	monoacid
	DBE=2-3, n_o=4	diacid/hydroxycarbonyl acid
	DBE = 1, n_o = 3−5 or DBE = 2, n_o>4	hydroxy acid
	DBE = 2, n_o = 3 or DBE = 3, $n_o \leq 6$	carbonyl acid
	DBE = 5 or 6, n_o = 2−5	aromatic acid
With N or S	n_N> 0, and n_S=0	nitrogen (N)-containing compounds (no S)
	n_S> 0, and n_N=0	sulfur (S)-containing compounds (no N)
	n_N> 0, and n_S>0	N and S-containing compounds

104

105

106

107

Reference

109   Gentner, D. R., Jathar, S. H., Gordon, T. D., Bahreini, R., Day, D. A., El Haddad, I., Hayes, P. L., Pieber, S. M., Platt, S. M., de Gouw, J.,
110   Goldstein, A. H., Harley, R. A., Jimenez, J. L., Prevot, A. S., and Robinson, A. L.: Review of Urban Secondary Organic Aerosol Formation
111   from Gasoline and Diesel Motor Vehicle Emissions, Environ Sci Technol, 51, 1074-1093, https://doi.org/10.1021/acs.est.6b04509, 2017.
112   Lambe, A. T., Ahern, A. T., Williams, L. R., Slowik, J. G., Wong, J. P. S., Abbatt, J. P. D., Brune, W. H., Ng, N. L., Wright, J. P., Croasdale,
113   D. R., Worsnop, D. R., Davidovits, P., and Onasch, T. B.: Characterization of aerosol photooxidation flow reactors: heterogeneous oxidation,
114   secondary organic aerosol formation and cloud condensation nuclei activity measurements, Atmos. Meas. Tech., 4, 445-461, 10.5194/amt-
115   4-445-2011, 2011.
116   Liu, S., Thompson, S. L., Stark, H., Ziemann, P. J., and Jimenez, J. L.: Gas-phase carboxylic acids in a university classroom: Abundance,
117   variability, and sources, Environmental Science & Technology, 51, 5454-5463, 2017.
118   Liu, T., Zhou, L., Liu, Q., Lee, B. P., Yao, D., Lu, H., Lyu, X., Guo, H., and Chan, C. K.: Secondary organic aerosol formation from urban
119   roadside air in Hong Kong, Environmental science & technology, 53, 3001-3009, https://doi.org/10.1021/acs.est.8b06587, 2019.
120   Peng, Z., Day, D. A., Ortega, A. M., Palm, B. B., Hu, W., Stark, H., Li, R., Tsigaridis, K., Brune, W. H., and Jimenez, J. L.: Non-OH
121   chemistry in oxidation flow reactors for the study of atmospheric chemistry systematically examined by modeling, 2016.
122   Watne, A. K., Psichoudaki, M., Ljungstrom, E., Le Breton, M., Hallquist, M., Jerksjo, M., Fallgren, H., Jutterstrom, S., and Hallquist, A.
123   M.: Fresh and Oxidized Emissions from In-Use Transit Buses Running on Diesel, Biodiesel, and CNG, Environ Sci Technol, 52, 7720-7728,
124   https://doi.org/10.1021/acs.est.8b01394, 2018.
125